1 Model Formulation

1.1 Physical Model

Our oceanic circulation model solves the so-called Primitive Equations in an Earth-centered rotating environment. They are based on the Boussinesq approximation (i.e. where density variations are neglected everywhere except in the gravitational force) and hydrostatic vertical momentum balance (*i.e.,* parallel to gravity) and are expressed in an Earth-centered, Cartesian system of coordinates rotating at an angular velocity $\vec{\Omega} = f(y)\vec{k}$:

$$
\begin{aligned}
\nabla \cdot \vec{u} + \frac{\partial w}{\partial z} &= 0 \\
\frac{D\vec{u}}{Dt} + 2f\vec{k} \times \vec{u} &= -\frac{1}{\rho_0}\nabla p - \frac{g\rho}{\rho_0}\vec{k} + \vec{F} \\
\frac{\partial p}{\partial z} &= -\rho g \\
\frac{DT}{Dt} &= D_T, \quad \frac{DS}{Dt} = D_S \\
\rho &= R(T,S,p).
\end{aligned}
\tag{1}
$$

Here (x, y, z) are the horizontal, vertical coordinates, $(\vec{u}, w)$ is the velocity, D/Dt is the so-called advective time derivative moving with the velocity, ρ is the density, p is the pressure, $\vec{k}$ is the vertical unit vector, ρ_0 is the mean density, g is the acceleration of gravity, T is the temperature, S is the salinity, and R is the oceanic equation of state. $\vec{F}$ and D represent the non-conservative effects of unresolved small-scale turbulence. ROMS is discretized in coastline- and terrain-following curvilinear coordinates.

The boundary conditions for the model are appropriate for an irregular solid bottom and coastline, free upper surface, and open-ocean sides away from the coastline. These include the forcing influences of surface wind stress and heat and water fluxes, coastal river inflow, bottom drag, and open-ocean outgoing wave radiation and nudging towards the specified basin-scale circulation. Applying ROMS to the North American west-coastal ocean has the requirement of obtaining well-behaved, long-term solutions for coastal configurations with **open boundaries** on up to three sides, through which the influences of the large-scale, external circulation must be conveyed. As part of the means of achieving this, we have devised a new radiation boundary scheme which estimates a two-component, horizontal phase velocity near the open boundaries, *cf.,* [Raymond & Kuo 1984, Barnier *et al.*1998]; however, unlike in other prototypes, we discretize both normal and tangential propagation in an upstream-biased fashion, where the normal component is treated implicitly. This method escapes the usual difficulties associated with large phase speeds and small-scale noise, hence it allows large time steps without loss of stability. No enhanced dissipation is needed near the boundary (*i.e.,* "sponge layers") to maintain numerical stability. Large-scale influences are implemented with nudging bands along the open boundaries, where all fields are relaxed toward specified data (which come from observations or a larger domain, coarse resolution model). The nudging rate is adjusted dynamically depending on inward/outward propagation of information as determined by the radiation algorithm. This method allows the avoidance of long term drifts (a typical consequence of unforced radiation boundary conditions, which are numerically stable, but fail to supply correct large-scale information) and an over-specification problem (typically manifested by spurious currents along open boundaries in the case of excessive nudging on outflow side; *cf.,* [Miyakoda & Rosati 1977]). A paper has been published on this new method, [Marchesiello *et al.*2001].

The modeling choices for $\vec{F}$ and D have important influences on the simulated coastal circulation. Oceanic material transports remain nearly within isopycnal surfaces (*i.e.,* with constant density) except in boundary layers, and small-scale parameterizations that respect this constraint yield substantial benefits [Gent & McWilliams 1990, Danabasoglu *et al.*1994, Griffies *et al.*1998]. It is especially challenging to limit spurious cross-isopycnal diffusion with a terrain-following vertical coordinate, since the intersection angle between coordinate and isopycnal surfaces is generally larger than with a z-coordinate model. We improved this behavior in ROMS with a variable-stencil, **isopycnal-transport** scheme that dynamically aligns its stencil with the isopycnal surfaces and reduces the extent of the stencil in the cross-isopycnal direction. The atmospheric responses and biological coupling both require skillfully parameterized **vertical mixing** in the interior and Planetary Boundary Layers (PBL). We have implemented a non-local, K-profile PBL scheme [Large *et al.*1994] that performs well in both data comparisons and large-domain model solutions [Li *et al.*2001], adapted to the C-grid structure of ROMS. A further extension of this scheme to the bottom boundary layer is now also in ROMS, with demonstrable benefits in shallow water near shore. Thus, D is determined by these two parameterization schemes, as is the vertical flux-divergence contribution to $\vec{F}$; the horizontal flux-divergence part of $\vec{F}$ is discussed in the next section as part of the advection algorithm.

1.2 Numerical Methods

Similar to other oceanic models (*i.e.,* POM, MICOM, POP, and SCRUM; [Blumberg & Mellor 1987, Bleck & Smith 1990, Killworth *et al.*1991, Song & Haidvogel 1994]), ROMS is a *split-explicit, free-surface* ocean model, where short time steps are used to advance the surface elevation and barotropic momentum, with a much larger time step used for temperature, salinity, and baroclinic momentum. Unlike these other models, however, ROMS employs a special 2-way time-averaging procedure for the barotropic mode, which satisfies the 3D continuity equation exactly in a finite-volume/finite-time-step sense. This permits us to construct 3D tracer fluxes which guarantee exact *volume-conservation* and *constancy-preservation*, *cf.,* [Leonard *et al.*1996, Shchepetkin & McWilliams 2002b]; whereas previous barotropic-baroclinic mode-splitting schemes can satisfy only one of these properties with the other one holding only to within the order of discretization accuracy. This feature removes a previous restriction to small sea-level changes relative to the unperturbed depth, which allows the model to retain numerical stability under numerically stiff conditions, such as strong tides (Sec. 1.7). The time-averaging procedure uses a temporal filter which is optimized for accuracy and stability by making the 3D time-step increments of amplitude and phase for oscillations associated with time-averaged barotropic mode and 3D time-step increments for baroclinic mode consistent within the range of frequencies resolved by 3D time-step (*i.e.,* barotropic mode filter "simulates" truncation error of baroclinic time stepping, [Shchepetkin & McWilliams 2002b]; also see [Higdon & Bennett 1996, Higdon & de Szoeke 1997, Hallberg 1997, Nadiga *et al.*1997]).

The **time-stepping algorithm** in ROMS allows a substantial increase in the permissible time-step size [Shchepetkin & McWilliams 2002b]. This is achieved by a specially designed predictor-corrector time step, where once the velocity is computed for the new sub-step (predictor or corrector), it is immediately used for the computation of tracers, and *vice versa*, with similar properties for the sea level free-surface and barotropic momentum. This scheme closely couples the fields, suppresses computational modes, and has a dissipation-dominant truncation error for the physical mode (as opposed to a dispersion-dominant error of the commonly used leap-frog or forward-backward time steps). As a consequence ROMS yields physically meaningful (*i.e.,* smooth on the grid scale) vertical velocity fields, which is known to be difficult with a hydrostatic, primitive-equation ocean model. The expanded regime of stability allows a larger time step. Yet a further gain in computational efficiency comes from putting the relatively expensive transport parameterizations outside the predictor-corrector cycle, thus halving their computational cost.

Sigma-coordinate pressure-gradient error has been known as a notorious problem for terrain-following atmospheric and oceanic models [Gary 1973, Mesinger 1982, Mesinger & Janjic 1985, Haney 1991, Beckmann & Haidvogel 1993, Beckmann & Haidvogel 1997, Haidvogel *et al.* 1993, McCalpin 1994, Chu & Fan 1997, Chu & Fan 1998, Barnier *et al.* 1998, Lin 1998, Mellor *et al.* 1994, Mellor *et al.* 1998, Song 1998]. We have been working on it for the past two years and have now made significant progress [Shchepetkin & McWilliams 2002a]. The approach we found most successful is based on a reconstruction of both the density field and the physical-height z-coordinate as continuous functions of the transformed coordinates (horizontal and sigma), with subsequent analytic integration to compute the pressure-gradient force. This approach not only achieves a formally higher order of accuracy, but it also retains and expands to higher orders several important symmetries of the original POM Jacobian formulation, which is used as a prototype. In doing so we encountered and successfully solved several difficulties; for example, we were able to develop *monotonized*, high-order, polynomial reconstruction algorithms, which are crucial for retaining numerical stability of the model in cases where the vertical density gradient changes abruptly within two consecutive grid intervals (since spurious oscillations from the interpolation scheme effectively act as negative stratification). We further incorporate an important correction due to the compressibility of seawater by a redesign of the equation of state for use in models.

Once a grid resolution passes a certain threshold, with viscosity decreased accordingly, the simulated flow becomes turbulent (*e.g.,* Fig. 4). Extensive experience with computational fluid dynamics for turbulent flows shows that conventional, second-order, discretized advection schemes are not the optimal choice (weighing accuracy against computational cost) in comparison with higher-order schemes. In ROMS we have redesigned the **advection operator** to reduce dispersive errors and, consequently, excessive dissipation rates, thereby effectively boosting the resolution on a given grid [Leonard 1979, Leonard, & Niknafs, 1991, Leonard *et al.*1996, Farrow & Stevens 1995, Hecht *et al.*1995, Shchepetkin & McWilliams 1998].

1.3 Parallel Code Design and Performance

ROMS was created for *shared-memory* architectures and efficient *cache utilization*; recently it has been extended for *distributed memory* architectures. ROMS was designed to be a coarse-grained, shared-memory parallel code, which uses 2D partitioning of the model grid into subdomains that may be assigned to different processors. The number of subdomains does not have to be the same as the number of processors (as usually happens in MPI codes), but it rather is chosen to make the memory storage associated with a subdomain fit into the secondary cache (*e.g.,* in going to a larger problem, it can be advantageous to increase the number of subdomains, hence subdomains per processor, rather than increase the size of the same subdomains). Originally SGI/Cray Origin2000 was the primary target computer for ROMS. Later the code was ported to Sun Enterprise and was used efficiently on from 4 to 64 processors by several scientific groups. In summer 1999, it became apparent that future computing needs require more flexibility, and a decision was made to develop a *message-passing* version using MPI with the view of hybrid-regime (MPI + Open MP) capability. Validation of ROMS parallel performances show that both methods result in viable overall scaling. The similarity between the MPI and Open MP performances indicates that cache management has at least as much of an effect as the choice of parallelization methods.

1.4 Nesting

ROMS is discretized on a structured grid, so local refinement can be performed via nested grids (*i.e.,* fixed high-resolution local models embedded in larger coarse-grid models). The interactions between the two components are twofold: the lateral boundary conditions for the fine grid are supplied by the coarse-grid solution, while the latter is updated from the fine grid solution in the area covered by both grids [Blayo & Debreu 1999]. Our method for embedded gridding takes advantage of the AGRIF (Adaptive Grid Refinement in Fortran) package [Debreu & Blayo 1999]. AGRIF is a Fortran 90 package for the integration of adaptative mesh refinement (AMR) features within a finite difference numerical model, with the ability to manage an arbitrary number of embedding levels as well as to do solution-adaptive grid-refinement (which we do not use). The package is based on the use of pointers which minimizes the changes in the original numerical model.

A recursive integration procedure manages the time evolution for the child grids during the time step of the parent grids. It is illustrated on Fig. 1a. In order to preserve the CFL criterion, for a typical coefficient of refinement (*e.g.,* x3 for a 5 km grid embedded in a 15 km grid), for each parent time step the child must be advanced using a time step divided by the coefficient of refinement as many times as necessary to match the time of the parent. For a simple 2-level embedding, the procedure is as follows: advance the parent grid by one parent time step; interpolate the relevant parent variables in space and time to get the boundary conditions for the child grid; advance the child grid by as many child time steps as necessary to reach the parent model time; and update point by point the parent model by the more accurate values of the child model.

Fig. 1b also shows the relative positions of the grid points between the parent and the child grids. We have adapted the AGRIF embedding procedure to the barotropic-baroclinic time-splitting structure of ROMS. The parent-child coupling is done at each baroclinic time step with pointwise local preservation of the volume fluxes across the parent-child boundaries.

The embedding is currently being applied in two regions: the central upwelling region around Monterey Bay and the Southern California Bight where the coastline, islands, and topography are highly convoluted. The procedure has been tested around the former site first with 2 levels, for a large domain at 15 km resolution and an inner domain centered on the Bay at 5 km resolution [Penven *et al.*2002a]. Long term simulations have been made to obtain equilibria, and the inner solution has been compared to large-domain solution at 5 km resolution. The embedded solution shows no

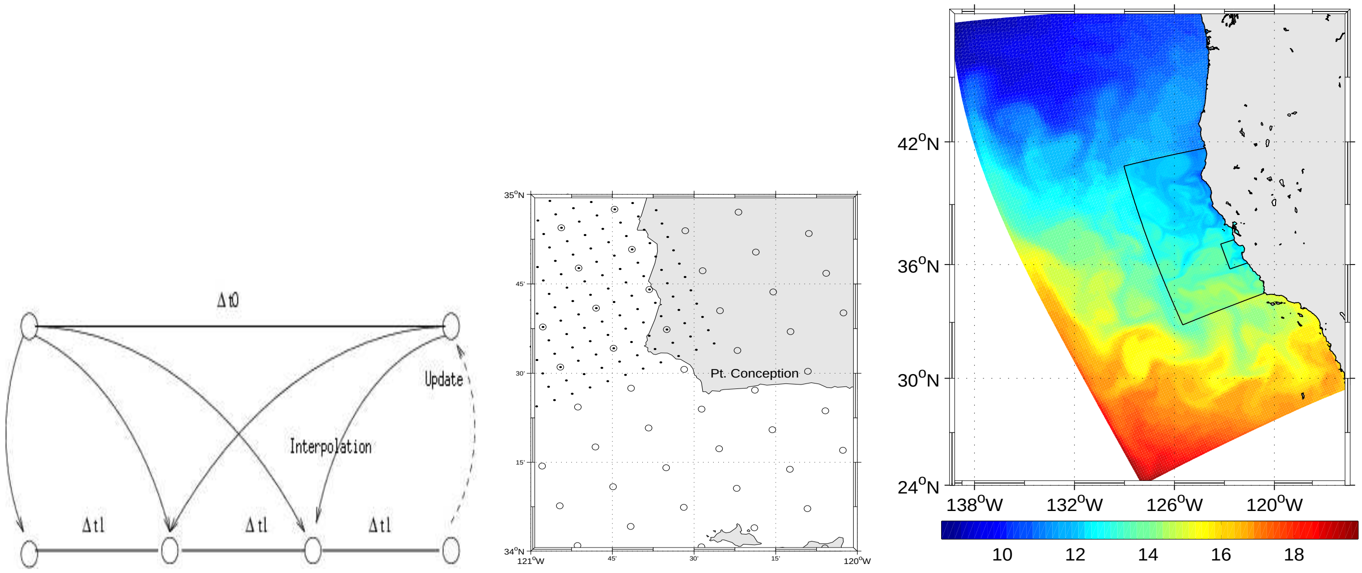

Figure 1: (Left) Temporal coupling between a parent-and-child grid and (middle) positions of the parent (o) and child (.) grid points around Point Conception for the 15+5km Monterey Bay simulation; The right panel shows sea surface temperature for this 15+5+1.5km Monterey Bay simulation, where the interfaces between parent and child grids are represented.

discontinuities at the parent-child domain boundary and a valid representation of the upwelling structure (Fig. 1b), at a CPU cost only slightly greater than for the inner region alone.

1.5 Biogeochemical Model

From its inception, ROMS has been intended to be a multi-purpose, multi-disciplinary oceanic modeling tool. A major aspect of our current focus is the investigation of biogeochemical cycling and ecosystem dynamics along the U.S. West Coast. We have presently incorporated a relatively simple upper ocean ecosystem model into ROMS. Such a model typically consists of the addition of several biogeochemical tracers that are advected and mixed by the model's transport schemes, undergo additional vertical movements either by sinking or specified behavioral motions, and interact with each other by biogeochemical transformations. Additionally, gaseous chemical species such as carbon dioxide are exchanged between sea and air depending on the respective partial pressures. The modularity of the ROMS code allows us to configure and explore different ecosystem model formulations, *e.g.,* [Fasham *et al.*1990, Frost 1993, Moisan & Hofmann 1996, Moore *et al.*2002]. What makes ROMS particularly suitable for such coupled physical-biological modeling is its K-Profile PBL surface boundary layer parameterization scheme (KPP) and its tolerance for highly stretched vertical grids (due to the vertical-spline discretization), used to efficiently enhance the resolution near the surface where most of the biological activity takes place. We currently are computing equilibrium U.S. West Coast (USWC) solutions with ecosystem dynamics and exploring the sensitivity to different model types, parameters, and resolution.

The ecosystem model that we are currently using for the USWC simulations is based on a single limiting nutrient (nitrogen) and incorporates only one phytoplankton and one zooplankton class. It nevertheless has eleven state variables: nitrate, ammonium, phytoplankton, zooplankton, small and large detritus (both nitrogen and carbon concentrations due to varying C:N ratios), oxygen, dissolved inorganic carbon, and total alkalinity. We also carry the ratio of chlorophyll to nitrogen in phytoplankton (θ) as a state-variable, in order to allow for photo-adaptation of phytoplankton and for evaluation of our computed phytoplankton fields with in situ or with remotely sensed observations of chlorophyll. The interactions of the eleven components of the ecosystem are shown in Fig. 2. The model includes explicit treatment of the subsurface light field; it particularly includes the additional attenuation of the downward penetrating light by phytoplankton adsorption. A further aspect that sets this model apart is its explicit treatment

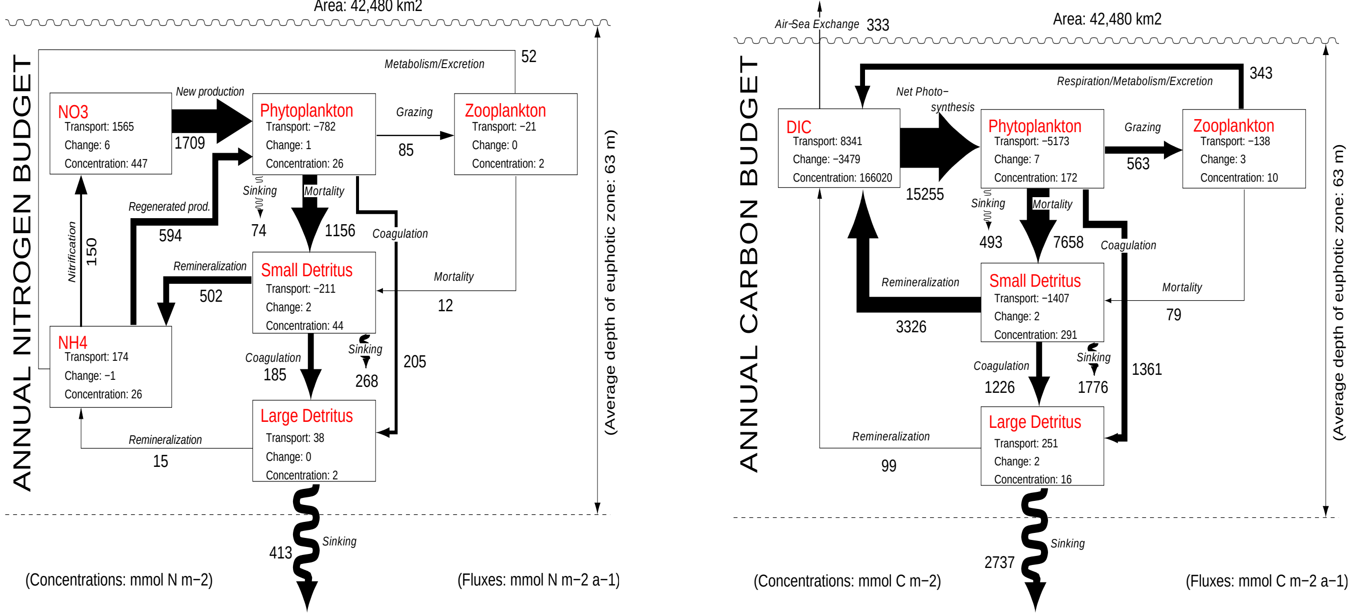

Figure 2: Schematic representation of the fluxes of nitrogen (left) and carbon (right) in the biogeochemical model. See section 4.1.2 for a further discussion of this figure.

of sinking for all particulate components.

1.6 Lagrangian Trajectories

in ROMS, the Primitive Equations are solved using spatial discretization where model variables are computed at fixed points (Eulerian approach). However, for physical as well as biogeochemical purposes, a description of oceanic processes in terms of particle trajectories can be very useful (Lagrangian approach). It basically requires the temporal integration of

$$\frac{d\vec{x}}{dt} = \vec{u}(\vec{x}, t), \tag{2}$$

providing an initial condition $\vec{x}(t_0) = \vec{x}_0$. Several algorithms have been developed to compute these trajectories off-line at moderate computational cost. In this case, the velocity field is stored periodically and used after completion of a run to estimate the velocities of the tracked particles. This method requires a time interval between data storage comparable to the time-scale of the dynamical problem being investigated. To take fully advantage of our high resolution solutions (which exhibit small-scale structures such as localized fronts and submesoscale eddies), we are implementing an on-line (parallelized) model for computing lagrangian trajectories. Eq. 2 is discretized in time, and velocities computed on ROMS grid are interpolated on-line to provide an accurate estimation of the right-hand side terms. In addition, a random turbulent vertical velocity term is computed to parameterize unresolved subgrid-scale phenomena along the vertical axis (in the horizontal directions, the effect of the subgrid scales is less significant and therefore neglected). To enhance computational efficiency, we are currently testing and developing the Lagrangian model including assessment of the performances of the numerical schemes. Eventually, the computational cost of the Lagrangian model should be very low (e.g. adding a single float is less costly than computing ROMS equations on one grid point in usual model configurations).

1.7 Water-quality Model

For water-quality modeling hydrodynamically passive tracer transport by advection and diffusion can be computed straightforwardly. Depending on the choice of the boundary and initial conditions for the tracers, residence times, turn-

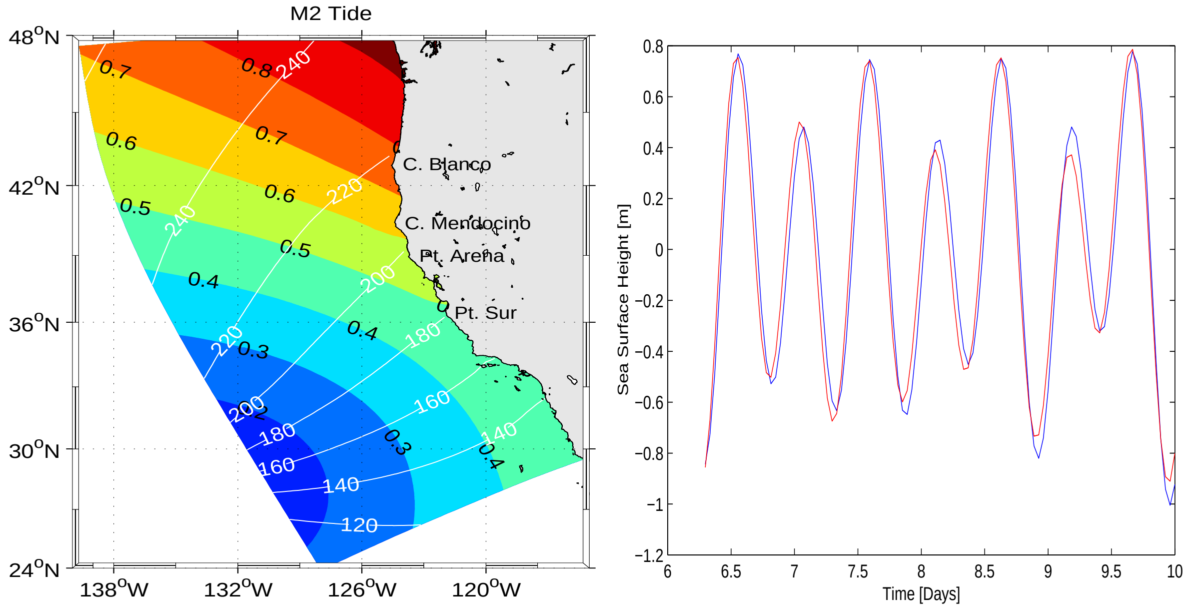

Figure 3: Left panel: M2 tidal amplitude and phase used to force the model in the USWC domain. Right panel shows a comparison between ROMS (blue line) and TXPO.5 (red line) solutions for the combined (M2,K1,S2,O1,N2) components. The barotropic tides in ROMS are able to generate tidal currents and internal tides on the shelf/slope region of Monterey Bay and in the Monterey canyon, benefiting from high resolution (1.5km) on the third-level, nested grid

over times and flushing times of designated subdomains can be determined from these model results to obtain additional quantitative information (*e.g.,* [Belluci *et al.*2001]). The calculation of age-concentrations (*cf.,* [Deleersnijder *et al.*2001]) can also be implemented.

1.8 Tidal Model

For tidal forcing, we use data from the OSU TOPEX/Poseidon Global Inverse Solution version 5.0 (TPXO.5). TPXO.5 is a global model of ocean tides, which best-fits, in a least-squares sense, the Laplace Tidal Equations and along track averaged data from TOPEX/Poseidon orbit cycles (Gary Egbert, Andrew Bennett, Michael Foreman, 1994: TOPEX/Poseidon tides estimated using a global inverse model, J. of Geophys. Res., vol99, No C12, pp. 24,821 - 24, 852). The tides are provided as complex amplitudes of earth-relative sea-surface elevation and tidal currents for eight primary harmonic constituents (M2, S2, N2, K2, K1, O1, P1, Q1), on a 1/2 degree resolution grid. These harmonics are introduced in ROMS through the open boundaries using the Flather condition (see Marchesiello et al., 2001). This open boundary condition combines the Sommerfeld equation (with surface gravity waves phase speed) with a 1-D version of the continuity equation applied in the outwardly normal direction at each open boundary:

$$\overline{u}_n = \overline{u}_n{}^{ext} - \sqrt{\frac{g}{h}}(\eta - \eta^{ext}), \tag{3}$$

where $\overline{u}_n$ is the normal component of barotropic velocity, η is the surface elevation, $\overline{u}_n{}^{ext}$ and η^{ext} represents the external data and h is the local water depth. In this equation the differences between the external data and the model predictions are allowed to propagate out of the domain at the speed of the external gravity waves. The volume is automatically conserved in the domain and variations due to physical forcing such as tides (but also the other subtidal components) are introduced through the external data.

ROMS solution with tidal forcing on the USWC domain are directly comparable to TPXO.5 (Fig. 3). The tidal signal for the region is a well known mixed (M2+S2/K1+O1), predominantly semi-diurnal tide. Differences between model and data never reach more than 10% for both amplitude and phase of each components (with maximum errors in the semi-diurnal M2 component), that is on the order of the differences given for TPXO.5 between TOPEX data and the solution for the Laplace Tidal Equations.

1.9 Sediment Model

ROMS already offered ample opportunity to address water quality issues by its capability to model tracer transport. Recently, however, the scope of ROMS has been extended further by the incorporation of suspended sediment transport. The sediments relate to the biogeochemical model mentioned above since the sea floor may act as a source or sink of carbon and nutrients. The sediments also relate to water quality since they may have contaminants adsorbed on them. Both the sediment transport and water quality modeling use ROMS's reliable tracer transport schemes. Various sediment size classes are modeled by tracers with a specified settling velocity.

Within ROMS point sources of tracers such as rivers, outfalls, and dump sites can be defined readily, but the major nonpoint source (or sink) of sediments is the sea floor. The exchange of material between the bed and water column is parameterized according to Smith and McLean [1977]: the resuspension flux of noncohesive suspended sediments is proportional to the excess of the bottom shear stress beyond a certain critical threshold value. This is still one of the most widely and successfully applied parameterizations (*e.g.,* see the test of various parameterizations by Garcia & Parker, 1991). A parameterization for cohesive sediments is to be implemented soon. Because of its role in the bottom sediment flux, accurate determination of the bed shear stress has become even more of an issue. Conditions where currents and waves combine are especially relevant in applications on the Californian Shelves. In addition to the existing wave-current bottom-boundary layer model [Styles & Glenn, 2000] we have implemented a parameterization of lower complexity [Soulsby, 1995], which is computationally less demanding. When using the sediment modules we not only enhance the vertical resolution near the sea surface, but also near the bottom, since the suspended sediment concentration profiles are predominantly confined in the lower part of the water column. For the same reason, the aforementioned extensions of the K-profile turbulence scheme to the bottom layer become especially relevant for accurate solution of vertical turbulent transport of sediment.

2 ROMS Applications to the Nearshore Regions off California

Over the last few years, our research has focused on the structure and dynamical mechanisms of regional and mesoscale physical variability in the California Current System (CCS) [Marchesiello *et al.*2002]. Studies of small, near-shore regions along the USWC require close coupling between the regional circulation and its local manifestations. A wide range of conditions can be found along the USWC, which forms a natural laboratory where coastal processes can be studied within an embedded grid approach. Although along-shore coastal winds are the dominant forcing from the northern tip of Washington (48°N) south to Point Conception (35°N) in Southern California, there is a significant difference north and south of 40N. During summer the along-shore winds are strongly favorable for coastal upwelling but are more variable north of 40°N. During winter low pressure systems from the Gulf of Alaska cause a strong northward component in the coastal winds and downwelling along the coast of Oregon and Washington, while upwelling generally continues intermittently in Central California (south of San Francisco, 37°N) interrupted by occasional winter storms. In the Southern California Bight (SCB), between Point Conception and the U.S.-Mexico Border, local winds are only a secondary forcing since interaction between remotely forced currents and bathymetry is dominant.

2.1 Water Quality in the Southern California Bight

The SCB forms a complex bathymetric region extending from the coast to 200 km offshore. Contrary to the California coast north of Point Conception, it is sheltered from the strong upwelling-favorable winds. As a result, the local circulation patterns are primarily driven by the interaction between bathymetry and remotely forced currents. A major problem in the heavily populated SCB is coastal water quality. A typical case is the situation at Huntington Beach (San Pedro shelf), where three years of beach postings and closures had consequences for public health, the state's image and its tourism industry. Two sources of pollution for coastal waters have been identified and opposed:

runoff from the storm drains and sewage plume. In the case of street runoff, surf zone dynamics is dominant in driving the fate of pollutants, but in the second case, it is believed that sewage water released a few miles at sea may show up in the surf zone, driven by the coastal circulation. A long-term goal is to use and develop ROMS to ultimately allow marine scientists to predict beach pollution (much as meteorologists warn of high air pollution). The local, small-scale dynamics in the SCB also set up an ideal case to be studied within the embedded domains. Up to now we have defined 3 levels of resolution: the first level is the 20km-grid USWC domain described above, parent of a second level which is a 6km-grid subdomain of the whole SCB, which in turn is the parent of the third level, a 2km-grid subdomain of Santa Monica Bay (SMB) and the adjacent Santa Monica-San Pedro channels and San Pedro Shelf.

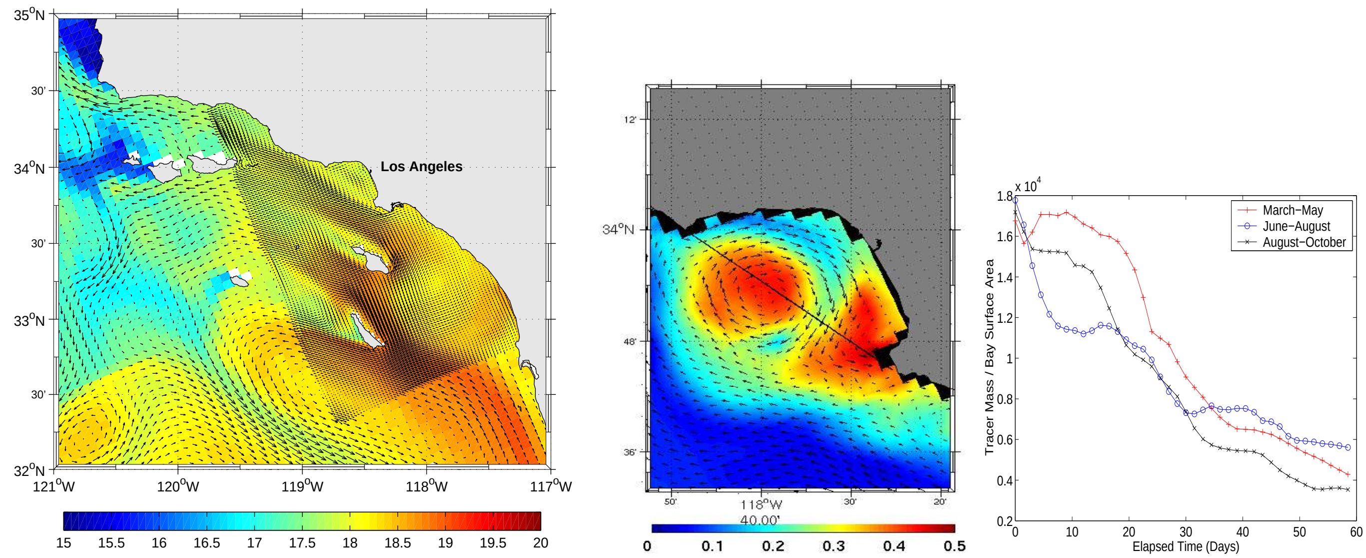

Figure 4: (a) Snapshot of surface temperature and currents on the fine grids of the 3-level embedded domains for the Southern California Bight studies; (b) Close up on Santa Monica Bay with a snapshot of the distribution of depth-integrated tracer concentration from the tracer tracking experiments. (residence time is computed for the area between the coastline and the straight line across the bay); (c) Time evolution of volume integrated tracer concentration (scaled by its initial value) for the 3 experiments.

We have done a multi-year simulation in one-way nesting mode until the solution equilibrated. The solution is qualitatively very comparable at the different levels, but the magnitude of currents increases with finer resolutions. The major current system is composed of the California Countercurrent flowing poleward along the coast in a cyclonic circulation. At the finest level we see that fluctuating currents within the bay and in the adjacent Santa Monica-San Pedro channels can be quite strong (up to 50 cm s^{-1}) relative to the climatological currents ($\sim$ 10 cm s^{-1}). These fluctuations are generated by disturbances of the mean currents interacting with coastline and topography and propagating poleward along the coast as coastal trapped waves (on time scales of a few days to a few weeks).

We have conducted a set of experiments in which a passive tracer was released on the Santa Monica and San Pedro shelves (all grid points within the 300 m isobath) and its subsequent spreading was tracked. Typical circulation regimes have been selected from the aforementioned multi-year simulations: one in which the flow through San Pedro Channel was equatorward and two in which this flow was opposite (often referred to as equatorward and poleward push [Hickey *et al.*2001]). During the poleward push a basin-wide anticyclonic circulation cell was present in the SMB, whereas during the equatorward push the flow through the SMB was more laminar. These different flow structures are expected to have a significant effect on the renewal of the shelf waters. To quantify this, the average residence time within the SMB has been calculated (see figure 4a-b for the area). [1] From this example it becomes clear that the more laminar flow (case 2, July in figure 4b) flushed the majority of the SMB relatively efficiently (τ_r = 12 days) whereas

[1]The average residence time is defined as $\tau_r = \int_0^\infty \tau\chi(t)\,dt$ where χ is the residence time distribution integrated over the volume of interest : $\chi(t) = \frac{-1}{\mathcal{N}_0}\frac{d}{dt}\mathcal{N}(t)$ with $\mathcal{N}$ the mass of tracer present within the basin at time = t and $\mathcal{N}_0$ the total mass initially present.

the presence of bay-scale anticyclonic eddies in the other cases cause the renewal to be slower ($\tau_r = 22$ and 18 days for case 1 and 3 respectively; figure 4c). Eddies slow down the flushing by retaining the tracer in the domain until they leave the area as whole, then taking the majority of the material with them. The snapshot of the tracer concentration in figure 4b shows the trapping of material within the eddy at the moment it is about to leave the domain. These results are generally consistent with the reports of sanitation groups monitoring bacterial surveys in Los Angeles county [City of Los Angeles, 1999], and the study by [Hickey *et al.*2001]. They also point out the importance of both remote forcing enabling the flushing and local eddies that effectively retain material on the shelf. The model allows us to study further the spatial characteristics of the observed disturbances, their generation process and their role in the flushing of the basins.

2.2 The Monterey Bay Configuration: results and prospects

The region of Monterey Bay (MB) is a large National Marine Sanctuary. The Monterey Bay Aquarium Research Institute (MBARI) is collecting chemical, biological and physical observations to be used by local, state and federal agencies for the management of harmful algal blooms, the advection and redistribution of pollution, and for long-term planning. Phytoplankton have greater variance at higher frequencies, as opposed to physical properties, so the coupled physical and biological ocean systems have responses that require measurements on the minute to decade and meters to 1000 km. Thus, in MBARI sampling strategies spatial coverage ultimately comes from observations made from space, but high-frequency temporal and vertical coverage come from moorings and drifters with arrays of *in situ* sensors. Based on these observations, the year was divided into four hydrographic periods: Upwelling (April-June); Oceanic-CUC (July-September); Early Davidson (October-November), and Late Davidson (December-March). Interestingly, the California Undercurrent (CUC), which occurs during the Oceanic-CUC Period, appears to transports the mesopelagic zooplankton (*Nanomia bijuga*) into Monterey Bay.

The 3-level embedded configuration of the Montery Bay region (with 1.5km resolution for the finest level) appears to be well-suited for its study. We propose in collaboration with MBARI researchers to investigate the general patterns and variability of physical and BGC properties around MB on daily to inter-annual time scales. We need to assess the role of the different forcings, including the canyon and surrounding capes and ridges, as well as local winds and remote forcing (e.g. associated to El-Niño induced coastal trapped waves). As a methodology we perform budget analyses, lagrangian trajectories and sensitivity experiments to resolution and topographic smoothness. Special emphasis is given to frontal instabilities (observed in our simulations provided the resolution is fine enough). As MB is a partly enclosed area, an important issue is water retention and residence time which is adressed by computing lagrangian trajectories or introducing numerical dyes (as for the Santa Monica bay area). At larger scales, we expect that the alongshore topographic variability in Central California constrains the alongshore structure of coastal upwelling and underlying biological activity. This hypothesis will be carefully checked particularly with regards to downscaling of these structures to the MB region. The use of lagrangian floats is very useful to provide estimates and patterns of transport, energy and potential vorticity export from the coastal margin to the open ocean. This will help to understand the interplay processes between coastal upwelling and offshore California Current System. Thus, we are trying to answer in relation with MBARI researchers an open question concerning alongshore variability of biological productivity, in particular areas of low coastal productivity despite conspicuous upwelling activity (e.g. south of Point Sur). The role of hydrodynamics will be confronted to the low iron supply hypothesis in which narrow shelf could display similar characteristics as open ocean systems.

We have first applied the embedding procedure to a domain that covers the central upwelling region of the USWC (around Monterey Bay) embedded into a domain including the whole USWC (Penven et al., 2002ab). We have obtained solutions for the central upwelling region at high resolution while preserving the large-scale circulation at affordable computational cost. This configuration was used to address uncertainties in the large-scale, low-frequency wind analyses used to force the model. Wind stress is recognized as the most important driving force for coastal upwelling while wind stress curl is the forcing term for large-scale transports in the Sverdrup balance equation. Our result shows that a correct representation of the wind stress curl at the shore is mandatory to obtain a realistic Davidson Current. Because COADS and NCEP are too coarse and because the scatterometer measurements of QuickSCAT can not be

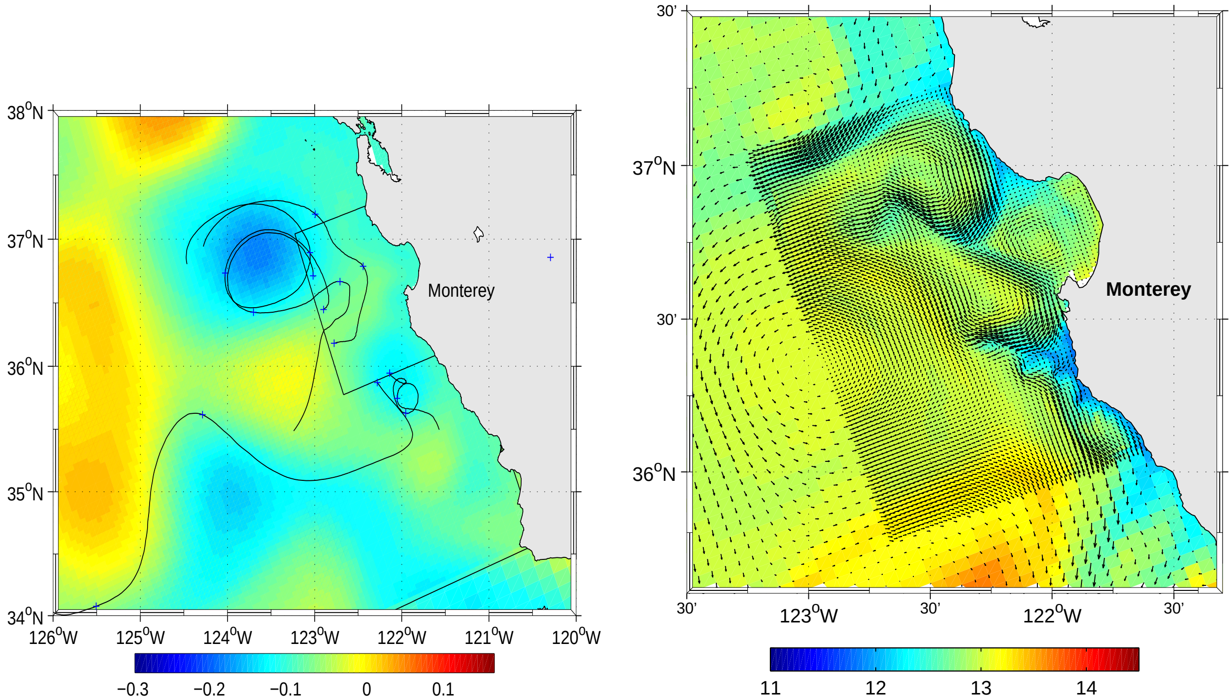

Figure 5: Left panel: Lagragian float trajectories released in the model's 3rd level grid (both in the interior and at the interface) and advected for a month, and mean SSH for the same summer month. The floats are able to cross the grid interface without obvious alteration. Note the dual aspect of these trajectories, where one group is advected and retained within a cyclonic mesoscale eddy while the other group is adveced quickly far offshore within an upwelling filament. Right Panel: Springtime Snapshot of surface temperature and currents. Note the small-scale frontal patterns along the cold filaments, and the participation of the mesoscale eddies in producing bay-scale eddies and connecting offshore waters with the water in the bay.

achieved in the vicinity of the coastline, this is solely accomplished by COAMPS. On the other hand, the experiments forced by QuickSCAT were the closest to the observations away from the shore. Based on these conclusions, we have worked in coordination with Yi Chao at JPL on a new blended product using both QuickSCAT and COAMPS data which should provide the oceanographic community with an optimal product for studying the CCS.

Model-data comparisons have revealed the limitations of the 5km grid resolution for local areas such as Monterey Bay, and the need for better defined coastline and topography (particularly the Montery Bay Canyon) as well as better resolved frontal dynamics interacting with these geographical features. To address these problems more precisely, we have added a 3rd-level grid at 1.5km resolution, embedded in the two parent levels (5km and 15km grids). Since pressure gradient errors are controled by smoothing topography at a given resolution, a net improvement with respect to topographic realism is obtained on the finest level in this particularly uneven area (compare isobaths at 5km and 1.5km on Fig. 6). Preliminary results show a corresponding improvement in pattern details over MB region, particularly regarding localized upwelling plumes (e.g. off Pt. Año Nuevo and Pt. Sur on Fig. 6), bay-scale eddies, and strong driving effects of the MB Canyon for water masses inside the bay.

In [Marchesiello *et al.*2002], we have seen that below 5km resolution, the model start producing an unstable mode pattern not present in the coarser simulations. It appears as a rapidly-growing, surface-trapped, short-wavelength frontal mode, similar to the ageostrophic, unstable modes described by McCreary *et al.*, (1991) and Barth (1994), associated by them with small-scale patterns commonly observed from satellite on upwelling fronts and jets in different coastal regions. Our results suggest the possibility of a transition regime as the grid resolution is enhanced where such frontal instabilities start to impact on coastal currents and offshore mesoscale eddies. An example of such small-pattern appears on Fig. 5 for the fineest grid level off Monterey.

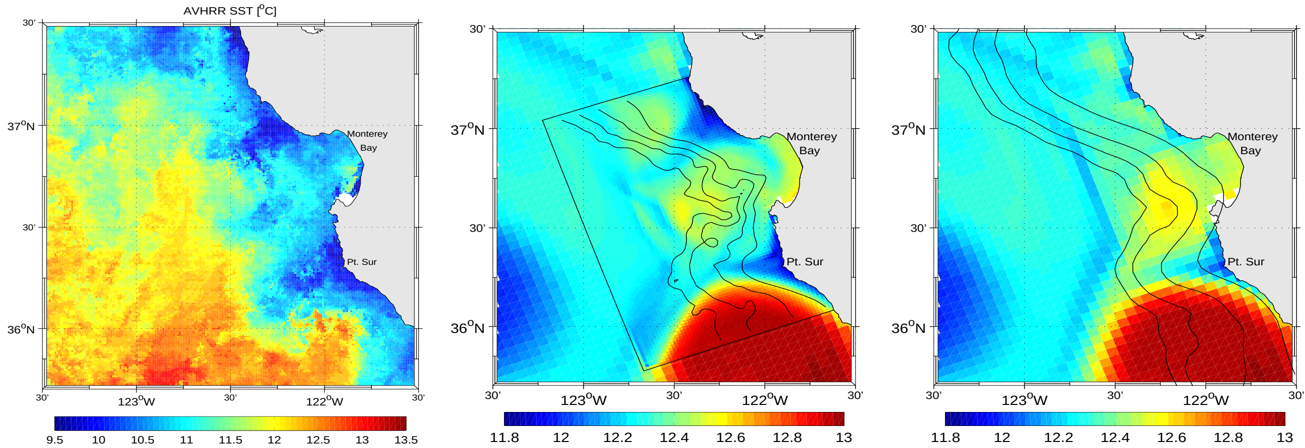

Figure 6: Satellite (left) and ROMS (middle and right) surface-layer temperature in May over Monterey Bay region. The model resolution is 5km (middle) or 1.5km within the box and 5km outside (right). The upwelling plumes off Pt. Año Nuevo and Pt. Sur are regularly observed in the MB region; they are also present in the model solutions but strongly enhanced and thus more realistic at fine resolution. Model 500m, 1000m, 1500m, and 2000m isobaths are shown for 1.5 and 5km resolution grids.

The nested approach is also particularly fruitful in stuying high-frequency phenomena such as local wind effects, internal tides, and phytoplankton production rates. We will be using the Blended QuickSCAT/COAMPS data to force the model with consistent local winds. Of particular interest in the area is the Monterey Bay canyon which was shown to concentrate and drive onshore an intense baroclinic tidal energy associated to vertical transport of denser water from within the canyon up onto the adjacent continental shelf [Petruncio *et al.*1998]. ROMS is capable of simulating such tidal process as it includes a tidal model (Sec. 1.7). The barotropic tides propagating from the boundaries along the USWC are able to generate internal tides in the model by interacting with the bottom topography. On the 3rd-level grid, the representation of the bottom topography and the resolution of the dynamical fields is fine enough that it allows realism in simulating internal tide generation ([Holloway 2001]). The fine resolution and non-linear dynamics resolved by ROMS is aslo permitting the generation of residual currents which are part of the shelf dynamics. We will be able to use the CODAR data in Monterey Bay to validate our results in this matter and possibly to be used in the assimilation scheme to improve predictability on the shelf.

References

[Barnier *et al.*1991] Barnier, B., B.L. Hua, and C. Le Provost, 1991: On the catalytic role of high baroclinic modes in eddy-driven large-scale circulations. *J. Phys. Ocean.*, **21**, 976-997.

[Barnier *et al.*1998] Barnier, B., P. Marchesiello, A.P. de Miranda, J.M. Molines, and M. Coulibaly, 1998: A sigma-coordinate primitive equation model for studying the circulation in the South Atlantic. Part I: Model configuration with error estimates. *Deep-Sea Res.*, **45**, 543-572.

[Barth 1994] Barth J.A., 1994: Short-wavelength instabilities on coastal jest and fronts. *J. Geophys. Res.*, **99**, 16095-16115.

[Beckmann & Haidvogel 1993] Beckmann, A., and D.B. Haidvogel, 1993: Numerical simulation of flow around a tall isolated seamount. Part. 1: Problem formulation and model accuracy. *J. Phys. Ocean.*, **23**, 1736-1753.

[Beckmann & Haidvogel 1997] Beckmann, A., and D.B. Haidvogel, 1997: A numerical simulation of flow at Fieberling Guyot. *J. Geophys. Res.*, **102**, 5595-5613.

[Belluci *et al.*2001] Bellucci, A. and G. Buffoni and A. Griffa and E. Zambianch, 2001: Estimation of residence times in semi-enclosed basins with steady flows. *Dyn. Atmos. Oceans*, **33**, 201-218.

[Blayo & Debreu 1999] Blayo, E. and L. Debreu, 1999: Adaptative mesh refinement for finite-difference ocean models: first experiments. *J. Phys. Ocean.*, **29**, 1239–1250.

[Bleck & Smith 1990] Bleck, R., and L.T. Smith, 1990: A wind-driven isopycnic coordinate model of the north and equatorial Atlantic Ocean: 1. Model development and supporting experiments. *J. Geophys. Res.*, **95C**, 3273-3285.

[Blumberg & Mellor 1987] Blumberg, A.F., and G.L. Mellor, 1987: A description of a three-dimensional coastal ocean circulation model. In *Three-dimensional Coastal Ocean Models*, ed. N. Heaps (Pub. AGU), pp. 1-16.

[Boehlert & Schumacher 1997] Boehlert, G.W., and J.D. Schumacher, 1997: *Changing oceans and changing fisheries: environmental data for fisheries research and management.* NOAA Technical Memorandum NMFS. NOAA-TN-NMFS-SWFSC-239.

[Cacchione *et al.*2002] Cacchione, D. A., and L. F. Pratson and A. S. Ogstond, 2002: The shaping of continental slopes by internal tides. *Science* **296**, 724-727.

[Chavez *et al.*2002] Chavez F., P. Strutton, G. Friederich, R. Feely, G. Feldman, D. Foley, M. McPhaden, 1999: Biological and chemical response of the equatorial Pacific ocean to the 97-98 El Niño, *Science*, **286**, 2126-2131.

[Cherniawsky *et al.*2001] Cherniawsky, J.Y., M.G.G. Foreman, and W.R. Crawford, 2001: Altimeter observations of sea level variability off the West Coast of North America. *Int. J. Rem. Sens.*, submitted.

[Chu & Fan 1997] Chu, P.C., and C. Fan, 1997: Sixth-order difference scheme for sigma coordinate ocean models. *J. Phys. Ocean.*, **27**, 2064-2071.

[Chu & Fan 1998] Chu, P.C., and C. Fan, 1998: A three-point combined compact difference scheme. *J. Comp. Phys.*, **140**, 370-399.

[City of Los Angeles, 1999] City of Los Angeles, Environmental Monitoring Division, 1999: Marine Monitoring in Santa Monica Bay: Biennial Assessment Report for the period January 1997 through December 1998 *Report submitted to EPA and RWQBC (Los Angeles)*, Department of Public Works, Bureau of Sanitation, Hyperion Treatment Plant, Playa del Rey, California, pp. 1-1 – 8-34 + appendices.

[Clyne, *et al.*, 1998] Clyne J., T. Scheitlin, and J.B. Weiss, 1998: Volume visualizing high-resolution turbulence computations, in *Theoretical and Computational Fluid Dynamics* (Springer-Verlag), 195.

[CoOP 1998] CoOP, 1998: Wind-driven transport science plan. *Coastal Ocean Processes (CoOP): Report Number 6.* UMCES-TS-170-98.

[Danabasoglu *et al.*1994] Danabasoglu, G., J.C. McWilliams, and P.R. Gent, 1994: The role of mesoscale tracer transports in the global ocean circulation. *Science* **264**, 1123-1126.

[Debreu & Blayo 1999] Debreu, L. and E. Blayo, 1999: AGRIF: Adaptive Grid Refinement in Fortran. *submitted to ACM Transactions on Mathematical Software - TOMS.*

[Deleersnijder *et al.*2001] Deleersnijder, E., and J.-M. Campin and E. J. M. Delhez, 2001: The concept of age in marine modelling. I: Theory and preliminary model results *J. Marine Systems*, **28**, 229–267

[Doney 1999] Doney, S.C., 1999: Major challenges confronting marine biogeochemical modeling, *Global Biogeochem. Cycles*,**13**, 705-714.

[Farrow & Stevens 1995] Farrow, D.E., and D.P. Stevens, 1995: A new tracer advection scheme for Bryan—Cox type ocean general circulation models. *J. Phys. Ocean.*, **25**, 1731-1741.

[Fasham *et al.*1990] Fasham, M.J.R., H.W. Ducklow, and S.M. McKelvie, 1990: A nitrogen-based model of plankton dynamics in the oceanic mixed layer. *J. Geophys. Res.*, **48**, 591-639.

[Frost 1993] Frost, B.W., 1993: A modeling study of processes regulating plankton standing stock and production in the open subarctic Pacific Ocean. *Prog. Oceanogr.* **32**, 17-56.

[Garcia & Parker 1991] Garcia, M., and G. Parker, 1991: Entrainment of Bed Sediment into Suspension. *J. Hydr. Eng.*, **117(4)**, 414-435.

[Gary 1973] Gary, J.M., 1973: Estimate of truncation error in transformed coordinate primitive equation atmospheric models. *J. Atmosph. Sci.*, **30**, 223-233.

[Gent & McWilliams 1990] Gent, P.R., and J.C. McWilliams, 1990: Isopycnal mixing in ocean circulation models. *J. Phys. Ocean.* **20**, 150-155.

[GLOBEC 1994] GLOBEC, 1994: Eastern boundary current program. A science plan for the California Current. *U.S. Global Ocean Ecosystems Dynamics. Report Number 11.*

[GLOBEC 1996] GLOBEC, 1996: U.S. GLOBEC Northeast Pacific Implementation Plan. *U.S. Global Ocean Ecosystems Dynamics. Report Number 17.*

[Griffies *et al.*1998] Griffies, S.M., A. Gnanadesikan, R.C. Pacanowski, V. Larichev, J.K. Dukowicz, and R.D. Smith, 1998: Isoneutral diffusion in a z-coordinate ocean model. *J. Phys. Ocean.*, **28**, 805-830.

[Haidvogel *et al.*1993] Haidvogel, D.B., A. Beckmann, D.C. Chapman, and R.-Q. Lin, 1993: Numerical simulation of flow around a tall isolated seamount: Part II: Resonant generation of trapped waves. *J. Phys. Ocean.*, **23**, 2373-3291.

[Haidvogel *et al.*2000] Haidvogel, D.B., H. Arango, K. Hedstrom, A. Beckman, P. Malanotte-Rizzoli, and A. Shchepetkin, 2000: Model evaluation experiments in the North Atlantic basin: simulations in nonlinear terrain following coordinates. *Dyn. Atmos. Oceans.* **32**, pp. 239-281.

[Hallberg 1997] Hallberg, R.W., 1997: Stable split time stepping schemes for large scale ocean modeling. *J. Comp. Phys.*, **135**, No. 1, pp. 54-65.

[Haney 1991] Haney, R., 1991: On the pressure gradient force over steep topography in sigma coordinate ocean models, *J. Phys. Ocean.*, **21**, 610-619.

[Hare & Mantua, 2000] Hare S. and N. Mantua, 2000: Empirical evidence for North Pacific regime shifts in 1977 and 1989, *Prog. Oceanogr.,* **47**, 103-146.

[Hecht *et al.*1995] Hecht, M., W.R. Holland, and P. Rasch, 1995: Upwind-weighted advection schemes for ocean tracer transport: An evaluation in a passive tracer context. *J. Geophys. Res.*, **100**, 20763-20778.

[Hickey 1992] Hickey, B.M., 1992: Circulation over the Santa Monica-San Pedro Basin and Shelf. *Prog. Oceanog.*, **30**, 37-115.

[Hickey 1998] Hickey, B.M., 1998: Coastal oceanography of western North America from the tip of Baja to Vancouver Island. In: *The Sea, the Global Coastal Ocean: Regional Studies and Syntheses* **11**, A.R. Robinson and K.H. Brink (eds.). Wiley, New York, 345-393.

[Hickey *et al.*2001] Hickey B.M., E.L. Dobbins and S.E. Allen, 2001: Currents and water properties of Santa Monica Bay and nearby basins. Submitted.

[Higdon & Bennett 1996] Higdon, R.L., and A.F. Bennett, 1996: Stability analysis of operator splitting for large-scale ocean modelling. *J. Comp. Phys.*, **123**, 311.

[Higdon & de Szoeke 1997] Higdon, R.L. and R.A. de Szoeke, 1997: Barotropic-Baroclinic Time Splitting for Ocean Circullation Modeling. *J. Comp. Phys.*, **135**, 31-53.

[Holland 1978] Holland, W.R., 1978: The role of mesoscale eddies in the general circulation of the ocean. Numerical experiments using a wind-driven quasi-geostrophic model. *J. Phys. Ocean.*, **8**, 363-392.

[Holloway 2001] Holloway, P.E. 2001: A regional model of the semi-diurnal internal tide on the Australian North West Shelf. *J. Geophys. Res.*, **106**, 19,625-.

[Killworth *et al.*1991] Killworth, P.D., D. Stainforth, D.J. Webb, and S.M. Paterson, 1991: The development of a free-surface Bryan-Cox-Semtner ocean model. *J. Phys. Ocean.*, **21**, 1333-1348.

[Large *et al.*1994] Large, W.G., J.C. McWilliams, and S.C. Doney, 1994: Oceanic vertical mixing: a review and a model with a non-local K-profile boundary layer parameterization. *Rev. Geophys.* **32**, 363-403.

[Leonard 1979] Leonard, B.P., 1979: A stable and accurate convective modelling procedure based on quadratic upstream interpolation, *Comput. Methods in Appl. Mech. Eng.,* **19**, 59-98.

[Leonard, & Niknafs, 1991] Leonard, B.P., and H. S. Niknafs, 1991: Sharp monotonic resolution of discontinuities without clipping of narrow extrema. *Comput. Fluids*, **19**141-154.

[Leonard *et al.*1996] Leonard, B.P., A.P. Lock and M.K. McVean, 1996: Conservative explicit unrestricted-time-step constancy preserving advection schemes. *Monthly Weather Review*, **124**, 2588-2606.

[Leonard & Niknafs 1991] Leonard, B.P. and H.S. Niknafs, 1991: Sharp monotonic resolution of discontinuities without clipping of narrow extrema. *Comput. Fluids.*, **19**, 141-154.

[Levitus *et al.*1994] Levitus, S., R. Burgett, and T.P. Boyer, 1994: World Ocean Atlas 1994. *NOAA Atlas NESDIS*, **3-4** U.S. Gov. Printing Office, Wash., D.C., 99 pp.

[Li *et al.*2001] Li, X., Y. Chao, J.C. McWilliams, and L.-L. Fu, 2001: A comparison of two vertical mixing schemes in a Pacific Ocean General Circulation Model. *J. Climate*, **14**, 1377-1398.

[Lin 1998] Lin, S.-J., 1998: A finite volume integration method for computing pressure gradient force in general vertical coordinates. *Q. J. R. Meteorol. Soc.,*, **123**, 1749-1762.

[Liu *et al.*1994] Liu, X.-D., S. Osher, and T. Chan, 1994: Weighted essentially non-oscillatory schemes, *J. Comp. Phys.*, **115**, 200-212.

[Liu *et al.*1994] Liu, K.-K., L. Atkinson, C.T.A. Chen, S. Gao, J. Hall, R.W. Macdonald, L. Talaue McManus, & R. Quiñones, 2000: Exploring continental margin carbon fluxes on a global scale, *EOS, Trans. American Geophys. Union* **81**, 641-644.

[Lynn *et al.*1995] Lynn, R.J., F.B. Schwing, and T.L. Hayward, 1995: The effect of the 1991-1995 ENSO on the California Current system. *CalCOFI Report 36*, 57-71.

[McCalpin 1994] McCalpin, J.D., 1994: A comparison of second-order and fourth-order pressure gradient algorithms in a σ-coordinate ocean model. *Int. J. of Num. Meth. in Fluids*, **18** , 361-383.

[McCreary *et al.*1991] McCreary J.P., Y. Fukamachi, and P.K. Kundu, 1991: A numerical investigation of jets and eddies near an eastern ocean boundary. *J. Geophys. Res.*, **96**, 2515-2534.

[Malanotte-Rizzoli *et al.*2000] Malanotte-Rizzoli, P., K. Hedstrom, H. Arango, and D. B. Haidvogel, 2000: Water mass pathways between the subtropical and tropical ocean in climatological simulation of the North Atlantic Ocean circullation. *Dyn. Atmos. Oceans*, **32**, 331-371.

[Marchesiello *et al.*2001] Marchesiello, P., and J.C. McWilliams, and A. Shchepetkin, 2001: Open boundary conditions for long-term integrations of regional oceanic models. *Ocean Modelling* **3**, 1-20.

[Marchesiello *et al.*2002] Marchesiello, P., J.C. McWilliams, and A. Shchepetkin, 2002: Equilibrium structure and dynamics of the California Current System. *J. Phys. Ocean.*, in press.

[Mellor *et al.*1994] Mellor, G.L., T. Ezer and L.-Y. Oey, 1994: The pressure gradient conundrum of sigma coordinate ocean models. *J. Atmos. Oceanic Technology*, **1994**, 1126-1134.

[Mellor *et al.*1998] Mellor, G.L., L.-Y. Oey, and T. Ezer, 1998: Sigma coordinate pressure gradient errors and the seamount problem. *J. Atmos. Oceanic Technology*, **1998**, 1122-1131.

[Mesinger 1982] Mesinger, F., 1982: On the convergence and error problems of the calculation of the pressure gradient force in sigma coordinate ocean models. *Geophys. Astrophys. Fluid Dyn.*, **19**, 105-117.

[Mesinger & Janjic 1985] Mesinger, F., and Z.I. Janjic, 1985: Problems and numerical methods of the incorporation of mountains in atmospheric models. *Lect. Appl. Math.*, **22**, 81-120.

[Miyakoda & Rosati 1977] Miyakoda, K., and A. Rosati, 1977: One way nested grid models: the interface condition and numerical accuracy. *Monthly Weather Review*, **105**, 1108-1118.

[Moisan & Hofmann 1996] Moisan, J.R., and E.E. Hofmann, 1996: Modeling nutrient and plankton processes in the California coastal transition zone 1. A time- and depth-dependent model. *J. Geophys. Res.*, **101**, 22647-22676.

[Moore *et al.*2002] Moore, J. K., S. C. Doney, J. A. Kleypas, D. M. Glover, and I. Y. Fung, 2002: An intermediate complexity marine ecosystem model for the global domain. *Deep-Sea Res. II*, **49**, 403-462.

[Nadiga *et al.*1997] Nadiga, B. T., M. W. Hecht, L. G. Margolin, and P. K. Smolarkiewicz, 1997: On Simulating Flows with Multiple Time Scales Using a Method of Averages. *Theor. and Comput. Fluid Dyn.*, **9**, 281-292.

[O'Reilly and Guza 1993] O'Reilly, W. C., and R. T. Guza, 1993: A comparison of two spectral wave models in the Southern Californian Bight. *Coast. Eng.*, **19**, 263–282.

[Pennington & Chavez, 2000] Pennington J. and F. Chavez, 2000: Seasonal fluctuations of Temperature, salinity, nitrate, chlorophyll and primary production at station H3/M1 over 1989-1996, *Deep-Sea Res.*, **47 II**, 947-973.

[Penven *et al.*2002a] Penven P., L. Debreu, P. Marchesiello, and J.C. McWilliams, 2002: Application and evaluation of the ROMS embedding procedure in the California Current System. *Ocean Modelling*, submitted.

[Penven *et al.*2002b] Penven P., P. Marchesiello, J.C. McWilliams, and Y. Chao, 2002: Coastal upwelling response to atmospheric wind forcing along the United States Pacific coast. *Journal of Physical Oceanography*, submitted.

[Petruncio *et al.*1998] Petruncio, E.T., L.K. Rosenfeld, and J.D. Paduan, 1998: Observations of the Internal tide in Monterey Canyon. *J. Phys. Ocean.*, **28**, 1873-1903.

[Ramp *et al.*1997] Ramp S., J. McClean, C. Collins, A. Semtner, K. Hays, 1997: Observations and modeling of the 91-92 El Niño signal off central California, 1997: *J. Geophys. Res.,* **102,** 5553-5582.

[Raymond & Kuo 1984] Raymond, W.H., and H.L. Kuo, 1984: A radiation boundary condition for multidimensional flows. *Q. J. R. Meteorol. Soc.,*, **110**, 535-551.

[Roemmich & McGowan 1995] D. Roemmich and J. McGowan, 1995: Climatic warming and the decline of zooplankton in the California current, *Science*, **267**, 1324-1326.

[Royer 1998] Royer, T.C., 1998. Coastal processes in the northern North Pacific. In: *The Sea, the Global Coastal Ocean: Regional Studies and Syntheses* **11**, A.R. Robinson and K.H. Brink (eds.). Wiley, New York, 395-414.

[Sanford & Maa 2001] Sanford, L. P., and J. P.-Y. Maa, 2001: A unifed erosion formulation for fine sediments. *Mar. Geol.*, **179**, 9–23.

[Skamarock & Klemp 1992] Skamarock, W.C., and J.B. Klemp, 1992, The stability of time-split numerical methods for the hydrostatic and the nonhydrostatic elastic equations. *Monthly Weather Review*, **120**, 2109–2197.

[Shchepetkin & McWilliams 1998] Shchepetkin, A., and J.C. McWilliams, 1998: Quasi-monotone advection schemes based on explicit locally adaptive dissipation. *Monthly Weather Review*, **126**, 1541-1580.

[Shchepetkin & McWilliams 2002a] Shchepetkin, A.F., and J.C. McWilliams, 2002a: A Method for computing horizontal pressure-gradient force in an oceanic model with a non-aligned vertical coordinate. *J. Geophys. Res.*, in press.

[Shchepetkin & McWilliams 2002b] Shchepetkin, A., and J.C. McWilliams, 2002b: Regional Ocean Modeling System: Development of a split-explicit, free-surface, topography-following coordinate ocean model. *Preprint.*

[da Silva *et al.*1994] da Silva, A., C. Young, and S. Levitus, 1994: Atlas of Surface Marine Data 1994, Vol. 1-5. *NOAA Atlas NESDIS* **6-10**. U.S. Gov. Printing Office, Wash., D.C.

[Smith & McLean 1977] Smith, J. D., and S. R .McLean, 1977: Spatially averaged flow over a wavy bed *J. Geophys. Res.*, **82**, 1735–1746.

[Smith & Hollibaugh 1993] Smith, S.V., & J.T. Hollibaugh, 1993: Coastal metabolism and the oceanic organic carbon balance, *Rev. Geophys.* **31**, 75-89.

[Smolarkiewicz & Grabowski 1990] Smolarkiewicz, P.K., and W.W. Grabowski, 1990: The multi-dimensional positive-definite advection transport algorithm: Nonocsillatory option. *J. Comp. Phys.*, **86**, 355-375.

[Song & Haidvogel 1994] Song, Y.T., and D.B. Haidvogel, 1994: A semi-implicit ocean circulation model using a generalized topography following coordinate system. *J. Comp. Phys.*, **115**, 228-248.

[Song, 1998] Song, Y. T., 1998: A General Pressure Gradient Formulation for Ocean Models. Part I: Scheme Design and Diagnostic Analysis, *Monthly Weather Review*, **126**, 3213-3230.

[Song & Wright, 1998] Song, Y. T., and D. G. Wright, 1998: A General Pressure Gradient Formulation for Ocean Models. Part II: Energy, Momentum and Bottom Torque Consistency, *Monthly Weather Review*, **126**, 3213-3230

[Soulsby, 1995] Soulsby, R. L, 1995: Bed shear-stresses due to combined waves and currents on the continental shelf. In M. J. F. Stive and H. J. de Vriend and J. Fredsøe and L. Hamm and R. L. Soulsby and C. Teisson and J. C. Winterwerp, *Advances in Coastal Morphodynamics*, Wiley, pp. 4-20–4-23

[Styles & Glenn, 2000] Styles, R., and S. M. Glenn, 2000: Modeling stratified wave and current bottom boundary layers on the continental shelf, *J. Geophys. Res.*, **105(C10)**, 24119-24139

[Walsh 1991] Walsh, J.J., 1991: Importance of continental margins in the marine biogeochemical cycling of carbon and nitrogen, *Nature* **350**, 53-55.

[Wiberg *et al.*2002] Wiberg, P. L., and D. E. Drake and C. K. Harris and M. Noble, 2002: Sediment transport on the Palos Verdes shelf over seasonal to decadal time scales. *Cont. Shelf Res.*, **22**, 987–1004.

[Yavneh *et al.*1997] Yavneh, I., A.F. Shchepetkin, J.C. McWilliams and, L.P. Graves, 1997: Multigrid Solution of Rotating, Stably Stratified Flows: The Balance Equations and Their Turbulent Dynamics; *J. of Comp. Phys.*, **136**245-262.

[Zalesak 1979] Zalesak, S.T., 1979: Fully multi-dimensional flux-corrected transport algorithms for fluid. *J. Comp. Phys.*, **31**, 335-362.